HYDROGEOCHEMICAL AND MICROBIOLOGICAL ASSESSMENT OF GROUNDWATER IN AN UNSERVED URBAN DISTRICT OF CHAD

Hammadou ABDOU[1], Moustapha DINAR IBRAHIM[1]*, Abdelhamid MAHAMAT ISSA[2], Mahamat Nour ABDELHAKH SAFI[2], Charles LAOKOURA[3]

[1]*Department of Geology, Faculty of Sciences and Technics, Adam Barka University of Abéché, Abéché, Chad*

[2]*Department of Chemistry, Faculty of Sciences and Technics, Adam Barka University of Abéché, Abéché, Chad*

[3]*Laboratoire de Géosciences et Développement Durable, Département des Sciences de la Terre, Université de Maroua, Cameroon*

**Correspondence: Moustapha Dinar Ibrahim (moustaphadinard@gmail.com, +235 66 001394)*

Abstract:

Groundwater is a vital source of drinking water in arid sub-Saharan Africa, but its quality is threatened by both natural mineralization and anthropogenic contamination. This study assesses the hydrogeochemical and microbiological quality of groundwater in unserved urban neighborhoods of Abéché, Chad, where residents depend on shallow wells and boreholes. Sixteen samples collected in dry and wet seasons 2023 were analyzed for physicochemical and bacteriological parameters. Results show slightly basic pH (6.3-7.7), variable electrical conductivity (61-2900 µS/cm), and total dissolved solids (55-2030 mg/L), with dominant Ca-Mg-HCO_3 facies reflecting carbonate and silicate weathering. Principal component analysis (PCA) indicates that water-rock interactions (42.3% of variance) are the primary mineralization driver, followed by anthropogenic inputs (21.4% from NO_3^- and Cl^-). Seasonal differences (higher EC in dry season, $p < 0.01$) highlight evaporation effects. Bacteriological analysis reveals 81% of samples exceed WHO limits for total coliforms (up to 1.6×10^4 CFU/100 mL) and 38% for *Escherichia coli* (up to 4.32×10^3 CFU/100 mL), indicating fecal pollution from nearby latrines and runoff. The chemical Water Quality Index (WQI) classifies 81% as chemically suitable, but integration of bacteriological data reduces fully safe water to 19%. Irrigation indices classify most samples as C2S1 (medium salinity, low sodium hazard), posing moderate risks for salt-sensitive crops. Geochemical modeling (saturation indices) confirms calcite near equilibrium and gypsum undersaturation, supporting geogenic control. Findings underscore chemical acceptability but severe microbiological vulnerability, urging sanitation improvements, well protection, and low-cost disinfection. This work provides a transparent, data-based foundation for sustainable water management in data-scarce arid regions, aligning with SDG 6.

Keywords: *groundwater quality, hydrogeochemistry, microbiological contamination, Chad*

ÉVALUATION HYDROGÉOCHIMIQUE ET MICROBIOLOGIQUE DES EAUX SOUTERRAINES DANS UN ARRONDISSEMENT URBAIN NON DESSERVI DU TCHAD

Résumé

Les eaux souterraines constituent une source vitale d'eau potable en Afrique subsaharienne aride, mais leur qualité est menacée à la fois par la minéralisation naturelle et la contamination anthropique. Cette étude évalue la qualité hydrogéochimique et microbiologique des eaux souterraines dans des quartiers urbains non desservis d'Abéché, au Tchad, où les habitants dépendent de puits peu profonds et de forages. Seize échantillons prélevés en saisons sèche et humide 2023 ont été analysés pour les paramètres physico-chimiques et bactériologiques. Les résultats montrent un pH légèrement basique (6,3–7,7), une conductivité électrique variable (61–2900 µS/cm) et des solides dissous totaux (55–2030 mg/L), avec un faciès dominant Ca–Mg–HCO_3 reflétant l'altération des carbonates et des silicates. L'analyse en composantes principales (ACP) indique que les interactions eau–roche (42,3 % de la variance) sont le principal moteur de

ISSN 3079-4463, e ISSN 3079-4471 https://grece-tchad.com

minéralisation, suivies des apports anthropiques (21,4 % provenant de NO_3^- et Cl^-). Les différences saisonnières (CE plus élevée en saison sèche, $p < 0,01$) mettent en évidence les effets de l'évaporation. L'analyse bactériologique révèle que 81 % des échantillons dépassent les limites de l'OMS pour les coliformes totaux (jusqu'à $1,6\times10^4$ UFC/100 mL) et 38 % pour Escherichia coli (jusqu'à $4,32\times10^3$ UFC/100 mL), indiquant une pollution fécale provenant des latrines voisines et du ruissellement. L'indice chimique de qualité de l'eau (IQE) classe 81 % comme chimiquement propres à la consommation, mais l'intégration des données bactériologiques réduit à 19 % la part d'eau totalement sûre. Les indices d'irrigation classent la plupart des échantillons en C2S1 (salinité moyenne, faible risque de sodium), posant des risques modérés pour les cultures sensibles au sel. La modélisation géochimique (indices de saturation) confirme que la calcite est proche de l'équilibre et le gypse sous-saturé, ce qui appuie un contrôle géogénique. Les résultats soulignent une acceptabilité chimique mais une vulnérabilité microbiologique sévère, appelant à des améliorations de l'assainissement, à la protection des puits et à une désinfection à faible coût. Ce travail fournit une base transparente et fondée sur les données pour une gestion durable de l'eau dans les régions arides où les données sont rares, en cohérence avec l'ODD 6.
Mots clés : *qualité des eaux souterraines, hydrogéochimie, contamination microbiologique, Tchad*

Introduction

Safe drinking water remains a challenge in arid sub-Saharan Africa, where over 26% lack safely managed access (WHO/UNICEF, 2025). In Chad, a landlocked Sahelian nation with renewable groundwater reserves of approximately 20 billion m^3 annually (Ministry of Water and Energy, Chad, 2022), urban shortages persist due to inadequate infrastructure from the Société Tchadienne des Eaux (STE). Abéché, the capital of Ouaddai Province in eastern Chad, exemplifies this, with a population of nearly 179,000 inhabitants (Institut National de la Statistique, Tchad, 2021). In precarious neighborhoods such as Djatinié, Amirié, and Amar, residents depend almost entirely on unregulated shallow hand-dug wells (depths 5-15 m) and community boreholes (20-50 m), which are highly vulnerable to seasonal fluctuations, geological influences, and human activities like unsewered latrines and waste disposal.

In the region's Precambrian basement aquifers (dominated by granites, gneisses, and migmatites), hydrogeochemical processes drive natural mineralization through interactions between infiltrating rainwater and crystalline rocks, leading to elevated concentrations of calcium (Ca^{2+}), magnesium (Mg^{2+}), and bicarbonate (HCO_3^-) (Abderamane, 2016; Ngounou Ngatcha, 2011; Shuaibu et al., 2025). Typical groundwater in such settings exhibits pH 6.0-8.5, electrical conductivity (EC) 100-2000 µS/cm, total dissolved solids (TDS) <1000 mg/L (fresh), and nitrate (NO_3^-) <50 mg/L (WHO guideline), though variability arises from rock weathering and evaporation (Hem, 1985). Concurrently, anthropogenic pressures from rapid urbanization (including pit latrines within 10-50 m of abstraction points, solid waste dumps, and agricultural runoff) introduce nitrates, chlorides, and pathogens, compromising potability and posing health risks such as diarrheal diseases, which account for 15-20% of child mortality in Chad (WHO, 2022).

Previous studies in neighboring Sahelian countries highlight similar vulnerabilities: in Niger, Chippaux et *al.* (2002) reported widespread *E. coli* contamination in urban wells linked to fecal intrusion, while in Côte d'Ivoire, Koné (2005) attributed high salinity to silicate weathering in fractured aquifers. In Chad, assessments in areas like Moussoro (Diallo et *al.*, 2024) and Fitri (Bérest et al., 2024) documented moderate mineralization (EC 200-1500 µS/cm) but elevated coliforms (up to 10^4 CFU/100 mL), with localized Abéché studies (Nour et al., 2024) confirming 80-90% contamination rates in boreholes due to poor sanitation. Recent work in N'Djamena (Mahamat Al-hafiz Ousman et *al.*, 2024; Ousman et *al.*, 2024) further emphasizes hydrochemical and bacteriological challenges in urban settings. However, integrated hydrogeochemical and microbiological evaluations remain rare for Abéché's eastern districts, revealing a critical knowledge gap amid climate variability that intensifies recharge deficits (annual rainfall 338-652 mm) and contaminant mobilization (IPCC, 2022; WMO, 2025).

This paucity of comprehensive, transparent data hinders evidence-based policymaking, particularly for assessing potability (e.g., via Water Quality Index, WQI) and irrigation suitability (e.g., Sodium Adsorption Ratio, SAR), where high salinity can impair soil structure and crop yields (Ayers & Westcot, 1985). To address these gaps, the present study characterizes groundwater quality in Abéché's unserved districts, employing multivariate statistics (PCA) and geochemical modeling (saturation indices via PHREEQC) to unravel controlling processes (geogenic versus anthropogenic) while ensuring transparency through detailed methodological reporting, charge balance verification (<5% error), and alignment with WHO guidelines.

Specific objectives include: (1) quantifying physicochemical and bacteriological parameters with seasonal context; (2) identifying hydrochemical facies and mineralization mechanisms via Piper diagrams, PCA, and saturation indices; (3) evaluating potability using WHO-compliant WQI (Horton, 1965; Brown et *al.*, 1970) and irrigation indices (SAR, %Na, etc.); and (4) proposing targeted mitigation strategies informed by spatial correlations (e.g., latrine proximity). By bridging hydrogeochemistry with public health implications and providing full data traceability, this work contributes to sustainable water management frameworks in data-scarce arid environments, aligning with United Nations Sustainable Development Goal 6 (clean water and sanitation).

1. Materials and Methods

1.1 Study Area

Abéché (13°45'-13°49' N, 20°47'-20°50' E) is situated in the Sudanese-Sahelian transition zone of eastern Chad, at elevations of 537-567 m above sea level. The region experiences a semi-arid climate with bimodal rainfall (338-652 mm annually, peaking June-September), mean temperatures of 29°C, and potential evapotranspiration exceeding 2000 mm/year, yielding a negative water balance that limits recharge to ~10-20% of precipitation (Direction de la Meteorologie, Tchad, 2023; Vassolo et *al.*, 2023). Hydrographically, ephemeral wadis drain into the Chari-Logone basin, with limited perennial flow influencing shallow aquifer recharge rates estimated at 50-100 mm/year in fractured zones (Sambo et *al.*, 2023).

1.2. Hydrogeological Setting

Geologically, the area overlies Precambrian basement rocks, including granitic intrusions and migmatitic gneisses, weathered and fractured to form semi-confined aquifers with productivity of 1-5 L/s and transmissivity of 10^{-5}-10^{-3} m²/s (BRGM, 2010; Yacouba et *al.*, 2024). The weathering profile typically comprises a thin layer of lateritic soils (1-3 m), underlain by a saprolite zone (5-15 m thick) and fractured fresh bedrock. Groundwater occurs under unconfined to semi-confined conditions, with water table depths ranging from 5-15 m in shallow wells to 20-50 m in boreholes. Recharge occurs predominantly through direct infiltration of episodic rainfall along fracture networks and ephemeral wadis, with limited lateral runoff due to low topographic gradients. Discharge is mainly via evapotranspiration and baseflow to wadis during the wet season. Aquifer transmissivity supports low-yield abstraction, but vulnerability to surface contaminants is high in unconfined zones due to thin vadose layers and high fracture permeability. Soils are predominantly ferruginous tropical types (pH 6-8, organic matter <1%), highly erodible and contributing to ion leaching during rains. Vegetation consists of sparse *Acacia* savanna. Human dynamics amplify vulnerabilities: population density reaches ~5000 inhabitants/km² in informal settlements, with >70% relying on on-site pit latrines sited <50 m from water points, facilitating pollutant migration (UN-Habitat, 2022; Nour et al., 2024).

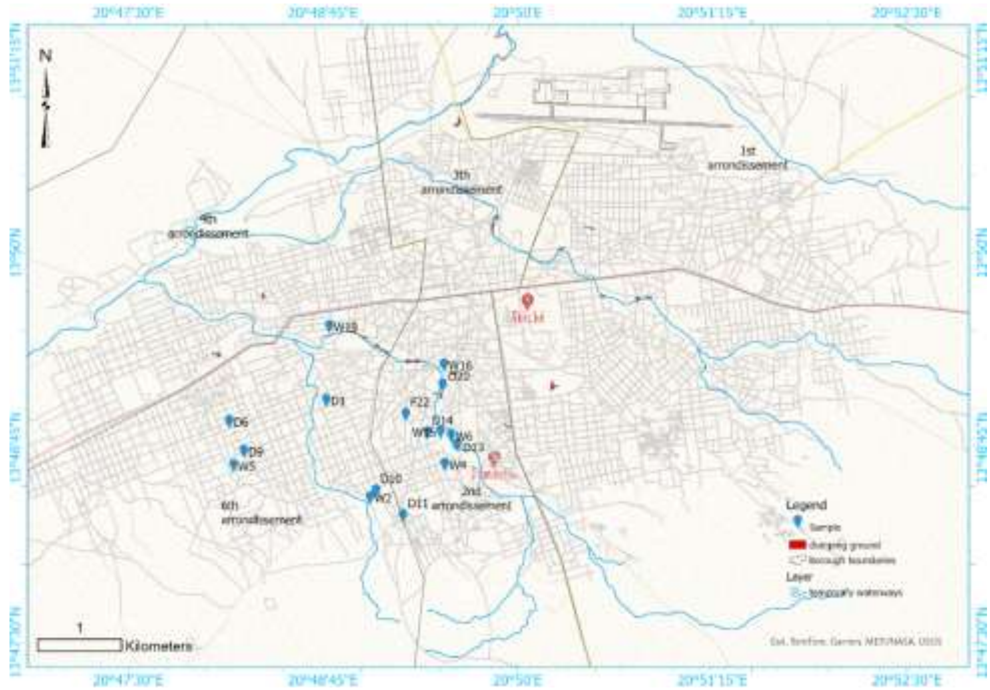

Figure 1 presents a plan-view map of sampling locations relative to wadis, urban extent, and the distribution of sanitation features (latrines) surveyed during fieldwork.

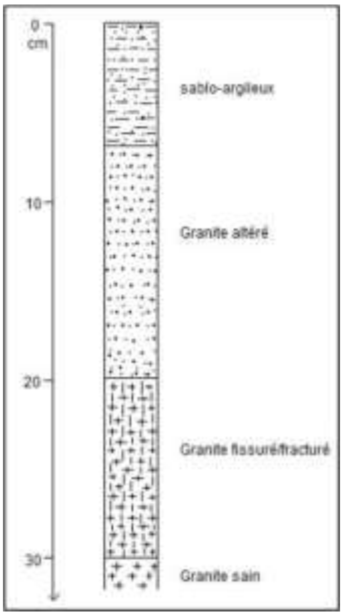

Figure 2 provides a conceptual hydrogeological profile along a NW-SE transect (A-A') through the neighborhoods Djatinié, Amirié, and Amar. The profile displays lithological units (lateritic soil, saprolite, fractured basement), water table positions in dry and wet seasons, abstraction structures (wells and boreholes), and potential contamination sources (latrines) with inferred infiltration pathways. The profile highlights the thin unsaturated zone beneath wells, the fractured zone tapped by boreholes, and the proximity of latrines to abstraction points.

1.3 Sampling Strategy

Sixteen groundwater sites were purposively selected across three precarious neighborhoods (Djatinié, Amirié, and Amar), based on community surveys for high-dependency areas lacking STE coverage and vulnerability hotspots (e.g., latrines/markets within 50 m). Criteria included: (i) exclusive reliance on the site (>50 households); (ii) absence of recent maintenance; and (iii) spatial coverage (kriging-informed grid ~500 m spacing). Seven shallow hand-dug wells (5-12 m depth) and nine boreholes (22-45 m) were sampled during March (dry season, low recharge, high residence time) and October (wet season, post-rainfall flushing) 2023, to capture seasonal variability. The same 16 sites were sampled in both seasons to enable paired statistical analysis. Coordinates were recorded via GPS (Garmin eTrex, ±3 m accuracy).

Prior to sampling, sites were purged of 3-5 borehole volumes (~100-300 L) to obtain stagnant-free groundwater, monitored via stabilized pH/EC (±5% change). Samples for physicochemical analysis were collected in 1-L high-density polyethylene (HDPE) bottles (acidified to pH < 2 with ultrapure HNO_3 for cation preservation); bacteriological samples in 500-mL sterile borosilicate glass bottles. All were double-bagged, transported on ice (<4°C), and analyzed at the National Water Laboratory (LNE), N'Djamena, within 24 hours, adhering to ISO 5667-11:2009 guidelines for groundwater sampling. Field blanks (deionized water) and duplicates (10% of samples) ensured quality control, with recovery rates >95%.

The sample size (n = 16) was determined by logistical constraints (remote access, vehicle/fuel costs) and budget, yielding ~70% statistical power to detect 20% differences in key parameters (EC, NO_3^-) at $\alpha = 0.05$ via power analysis (Faul et *al.*, 2007). This is a recognized limitation for fine-scale spatial inference but sufficient for facies identification and broad trends, consistent with similar Sahelian studies (n = 10-20; Diallo et al., 2024). To address potential biases from purposive selection (overrepresentation of contamination hotspots), geospatial analysis (GIS) was used to balance site distribution across vulnerability gradients, though minor selection bias may remain.

1.4 In Situ Measurements

Field parameters (temperature (T, °C), pH, electrical conductivity (EC, µS/cm), and dissolved oxygen (DO, mg/L)) were measured using a Hanna HI98130 portable multiparameter probe, calibrated daily against NIST-traceable standards (pH buffers 4.0/7.0/10.0; KCl 1413 µS/cm). Measurements stabilized after 2-3 minutes post-purge. Total dissolved solids (TDS, mg/L) were estimated in situ as $TDS \approx 0.7 \times EC$ (Hem, 1985), a semi-empirical factor for non-carbonate-dominated waters; lab-verified TDS (gravimetric evaporation) adjusted values by <10% for accuracy. DO calibration used Winkler titration equivalents.

1.5 Laboratory Analyses

1.5.1 Physicochemical Analyses

Major ions were quantified at LNE using validated methods (APHA, 2025; precision/replicate SD <5%). Cations: Ca^{2+} and Mg^{2+} via EDTA complexometric titration (0.01 M, eriochrome black T indicator, ±2 mg/L); Na^+ and K^+ by flame photometry (Jenway PFP7, air-acetylene flame, ±1 mg/L). Anions: HCO_3^- by acid titration (0.02 N HCl, phenolphthalein endpoint); Cl^- by argentometric titration ($AgNO_3$, ± 0.5 mg/L); SO_4^{2-} by UV-Vis spectrophotometry (Hach DR3900, barium chloride precipitation, 420 nm, ±5 mg/L); NO_3^- by cadmium reduction/colorimetry (540 nm, ±0.1 mg/L). Trace elements (Fe^{2+}, Mn^{2+}) via flame atomic absorption spectrometry (Varian AA240FS, ±0.01 mg/L) if above detection limit. Alkalinity was measured as HCO_3^- equivalents.

Ionic charge balance was calculated as $(\Sigma cations - \Sigma anions) / (\Sigma cations + \Sigma anions) \times 100$, with errors <5% for all samples, confirming dataset reliability (Appelo & Postma, 2005). All reagents were ACS-grade; lab blanks and spikes (e.g., 10 mg/L NO_3^-) recovered 98-102%. For TDS calculation, the sum of major ions (Ca^{2+}, Mg^{2+}, Na^+, K^+, HCO_3^-, Cl^-, SO_4^{2-}, NO_3^-) was used rather than the EC×0.7 estimate, following standard practice (APHA, 2025). The EC-based estimate was only used for field screening.

1.5.2 Bacteriological Analyses

Microbiological quality was evaluated per WHO (2011) and APHA (2025) using membrane filtration (0.45 µm, 47 mm). Total coliforms were enumerated on m-Endo agar (incubation 37°C/24 h, yellow colonies with sheen); *E. coli* confirmed on m-FC agar (blue colonies at 44.5°C/24 h, indole test). Aerobic mesophilic flora used Plate Count Agar (PCA, 35°C/48 h pour-plate). Volumes filtered: 100 mL (low counts) to 1 mL (high). Detection limit: 1 CFU/100 mL; method blanks (sterile water) were negative. Latrine distances (10-150 m) were GPS-measured for correlation. Incubators were validated (±0.5°C); duplicates (n = 3) showed <10% variability. No antibiotics/antiseptics interfered, per field questionnaire. The analysis focused on indicator organisms; future assessments could include additional pathogens for a more comprehensive risk profile.

1.6 Data Processing and Statistical Analysis

Hydrochemical facies were delineated using Piper trilinear and Stiff polygonal diagrams in AqQA software (v1.1.5; RockWare, 2012), plotting meq/L equivalents for visual ionic dominance. Geochemical processes (rock weathering vs. evaporation) were inferred from the relationships between major ions and TDS following the conceptual approach of Gibbs (1970), supported by principal component analysis. Geochemical indices included: total hardness ($TH = 2.5[Ca^{2+}] + 4.1[Mg^{2+}]$, mg/L as $CaCO_3$); saturation indices (SI) for calcite, dolomite, and gypsum were computed using PHREEQC v3.7.3 (Parkhurst & Appelo, 2013) with the MINTEQA2 database at 25°C; base exchange index ($BEI = Cl^- - (Na^+ + K^+)$, meq/L). Multivariate analysis employed PCA in PAST v4.03 (Hammer et al., 2001), with Z-score standardization and varimax rotation to extract factors with eigenvalues >1; loadings >0.7 were interpreted.

Potability was assessed via WQI (Horton, 1965; modified Brown et al., 1970):

$$WQI = \frac{\sum_{i=1}^{n} q_i w_i}{\sum wi}$$

where $q_i = 100 \times (C_i / S_i)$ (C_i = observed concentration, S_i = WHO standard) and $w_i = 1 / S_i$ (unit weight).Sub-indices qi were weighted for 11 parameters (pH, EC, TDS, major ions); thresholds: excellent (<50), good (50-100), poor (100-200), very poor (200-300), unsuitable (>300). To integrate bacteriological quality, total coliform counts were incorporated as an additional parameter. Given the absence of a numerical WHO guideline for total coliforms (standard requires 0 CFU/100 mL), a unit weight identical to that of unitless or qualitatively defined parameters was assigned (wi = 1). The sub-index for coliforms (q-coliform) was calculated using a semi-logarithmic scale that reflects order-of-magnitude increases in fecal contamination risk:

- 0 CFU/100 mL → q-coliform = 0 (excellent)
- 1-10 CFU/100 mL → q-coliform = 25
- 11-100 CFU/100 mL → q-coliform = 50
- 101-1000 CFU/100 mL → q-coliform = 75
- 1000 CFU/100 mL → q-coliform = 100 (unsuitable)

The bacteriological sub-index was incorporated with equal weight ($w_i = 1$) to other parameters, as recommended by Brown et al. (1970) for parameters without numerical guidelines. This progressive penalization ensures that even low contamination levels contribute to quality degradation without overly dominating the index when physicochemical parameters are compliant. The overall WQI was then computed as the weighted average of all 12 sub-indices. Additionally, samples were classified as "fully safe" for drinking only if both the physicochemical WQI and the bacteriological sub-index indicated "excellent" or "good" categories (i.e., overall WQI <100 and q-coliform ≤50). This dual criterion accounts for the overriding public health importance of microbial safety.

Irrigation suitability employed: Sodium Adsorption Ratio ($SAR = Na^+/\sqrt{[(Ca^{2+} + Mg^{2+})/2]}$), percent sodium ($\%Na = (Na^+ + K^+)/(Ca^{2+} + Mg^{2+} + Na^+ + K^+) \times 100$); permeability index ($PI = (Na^+ + \sqrt{HCO_3^-})/(Ca^{2+} + Mg^{2+} + Na^+) \times 100$); residual sodium carbonate ($RSC = (HCO_3^- + CO_3^{2-}) - (Ca^{2+} + Mg^{2+})$, meq/L); Kelly's ratio ($KR = Na^+ / (Ca^{2+} + Mg^{2+})$).

Classifications followed USSL (1954) SAR-EC diagrams (C1-C4 salinity, S1-S4 sodium hazard).

Spatial interpolation used ordinary kriging in ArcGIS v10.8 (Esri, 2023), with variogram modeling (spherical semivariogram, nugget 10%, sill 80%, range 1 km) fitted to EC/NO_3^- semivariograms ($n = 16$, cross-validation $R^2 = 0.75$). Normality was tested via Shapiro-Wilk; seasonal comparisons for paired samples (same sites, dry vs. wet season) were performed using the non-parametric Wilcoxon signed-rank test ($\alpha = 0.05$). Comparisons between independent groups (wells vs. boreholes) used the Wilcoxon rank-sum test. Correlations (Pearson's r for latrine distance vs.

NO_3^-/coliforms) assumed approximate normality post-log transformation. All computations in R v4.3.1 (R Core Team, 2023; packages: *factoextra* for PCA, *gstat* for kriging).

2. Results

2.1 Hydrochemical Characteristics and Facies

Groundwater temperatures ranged 26.5-32.1°C (mean 29.2 ± 1.8°C), reflecting shallow circulation influenced by ambient air (~28-30°C). pH values were near-neutral to slightly alkaline (6.3-7.7; mean 6.9 ± 0.4), within WHO limits (6.5-8.5) and indicative of carbonate buffering in basement lithology, with no significant seasonal difference ($p = 0.12$, Wilcoxon signed-rank test). EC varied widely (61-2900 µS/cm; mean 474 ± 600 µS/cm), exceeding the palatability threshold of 1500 µS/cm in 25% of samples—mostly dry-season wells (median 320 vs. 210 µS/cm wet; $p < 0.01$, Wilcoxon signed-rank test)—suggesting concentration via evaporation. TDS (calculated as sum of ions) mirrored EC trends (55-2030 mg/L; mean 332 ± 420 mg/L), classifying 75% as fresh (<1000 mg/L) and 25% brackish.

Major cations were dominated by Ca^{2+} (24-390 mg/L; mean 68 ± 100 mg/L) > Na^+ (4-460 mg/L; mean 53 ± 120 mg/L) > Mg^{2+} (12-74 mg/L; mean 14 ± 15 mg/L) > K^+ (2-40 mg/L; mean 12 ± 10 mg/L), accounting for 55-70% of meq/L equivalents and reflecting calcite/dolomite dissolution. Anions ranked HCO_3^- (21-432 mg/L; mean 144 ± 120 mg/L) > SO_4^{2-} (1-688 mg/L; mean 50 ± 150 mg/L) > Cl^- (1-265 mg/L; mean 21 ± 50 mg/L) > NO_3^- (0-22 mg/L; mean 5 ± 6 mg/L), with NO_3^- exceeding 50 mg/L in 19% (3 samples, all wells near latrines <20 m). DO levels (3.2-6.8 mg/L; mean 4.9 ± 1.2 mg/L) indicated oxic conditions, favoring nitrate stability over denitrification.

Table 1 summarizes physicochemical parameters.

Parameter	Min	Max	Mean ± SD	WHO Limit	% Exceeding
pH	6.3	7.7	6.9 ± 0.4	6.5-8.5	0
EC (µS/cm)	61	2900	474 ± 600	<1500 (palatable)	25
TDS (mg/L)	55	2030	332 ± 420	<1000	25
Ca^{2+} (mg/L)	24	390	68 ± 100	<200	0
Mg^{2+} (mg/L)	12	74	14 ± 15	<150	0
Na^+ (mg/L)	4	460	53 ± 120	<200	0
K^+ (mg/L)	2.0	40.0	12.0 ± 10.0	<12	0
HCO_3^- (mg/L)	21	432	144 ± 120	<300 (taste)	19
Cl^- (mg/L)	1.0	265.0	21.0 ± 50.0	<250	0
SO_4^{2-} (mg/L)	1.0	688.0	50.0 ± 150.0	<250	6
NO_3^- (mg/L)	0.0	22.0	5.0 ± 6.0	<50	0

Piper trilinear diagram (Figure 3) delineates a dominant Ca-Mg-HCO_3 facies in 75% of samples (earth-alkaline bicarbonate type), with secondary mixed Ca-Cl-SO_4 in high-EC wells (25%), indicating evaporation influence. Schoeller semi-log plots show logarithmic mineralization increase from boreholes (low EC ~200 µS/cm) to wells (~600 µS/cm), while Stiff polygons confirm elongated HCO_3^- dominance.

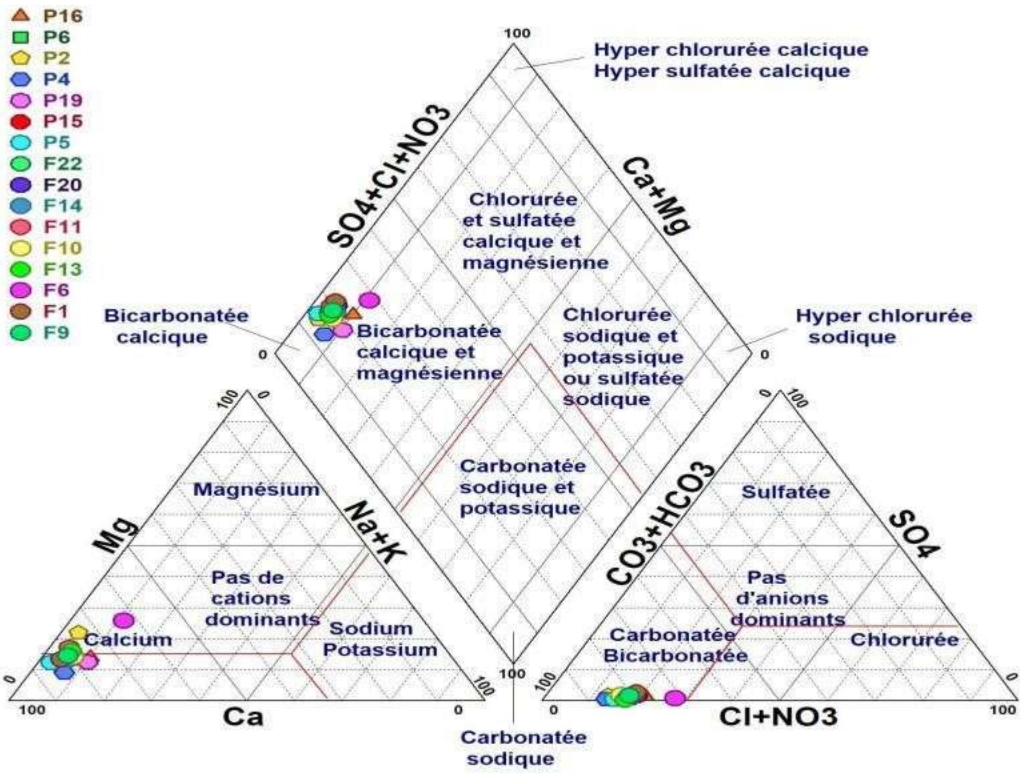

Figure 3. Piper trilinear diagram of groundwater samples (n = 16) showing dominant Ca-Mg-HCO_3 facies and a shift toward mixed Ca-Cl-SO_4 type in high-EC wells.

The dominant Ca-Mg-HCO_3 facies suggests rock weathering as the primary mineralization process. This interpretation is supported by the relationships between major ions and TDS, which indicate that 60-80% of samples fall within the rock-weathering domain when plotted on Gibbs diagrams (Gibbs, 1970), while approximately 20% of dry-season samples show an evaporation trend (Cl^-/HCO_3^- ratio >1). These observations are consistent with the PCA results (Factor 1: 42.3% variance, representing water-rock interaction) and the near-equilibrium saturation indices for calcite and dolomite (Table 2).

Total hardness (TH) ranged 120-350 mg/L as $CaCO_3$ (mean 220 ± 80 mg/L), classifying 56% as moderately hard (100-300 mg/L) and 44% as soft (<100 mg/L). **Saturation indices** (SI) calculated with PHREEQC are presented in Table 2. Calcite SI ranged from -0.1 to +0.8 (mean 0.4), indicating near-equilibrium to slight oversaturation; dolomite SI ranged from -0.2 to +0.6 (mean 0.2), also near equilibrium; gypsum SI were all negative (-2.5 to -1.2), indicating undersaturation. These values suggest that carbonate minerals control the solution chemistry, while gypsum dissolution is not a major source of ions. Base exchange index (BEI) values (-8 to +5 meq/L; mean -1.2) suggest minor cation exchange (Ca^{2+} for Na^+ in clay fractions), with negative values indicating calcite precipitation potential in high-Mg waters.

Table 2. Saturation indices for calcite, dolomite, and gypsum (n = 16)

Mineral	**Min**	**Max**	**Mean ± SD**
Calcite	-0.1	0.8	0.4 ± 0.3
Dolomite	-0.2	0.6	0.2 ± 0.2
Gypsum	-2.5	-1.2	-1.8 ± 0.4

2.2 Multivariate Statistics

PCA extracted three varimax-rotated factors explaining 75.6% of total variance (Kaiser-Meyer-Olkin = 0.82, Bartlett's $p < 0.001$). **Factor 1** (42.3% variance; eigenvalue 4.7) exhibited strong positive loadings (>0.8) for Ca^{2+}, Mg^{2+}, HCO_3^-, and SO_4^{2-}, representing water-rock interaction (carbonate/silicate weathering). **Factor 2** (21.4% variance; eigenvalue 2.4) showed high loadings for NO_3^- (0.85) and Cl^- (0.78), clearly identifying anthropogenic pollution from onsite sanitation. **Factor 3** (11.9% variance; eigenvalue 1.3) had moderate loadings for Na^+ (0.72) and K^+ (0.65), likely reflecting ion exchange and evaporation. **The PCA biplot (Figure 4)** illustrates sample distribution along these factors. Factor 1 correlated positively with depth ($r = 0.68$, $p < 0.01$), and Factor 2 correlated negatively with distance to the nearest latrine ($r = -0.72$, $p < 0.05$; log-transformed data), suggesting a link between contamination and proximity to sanitation facilities.

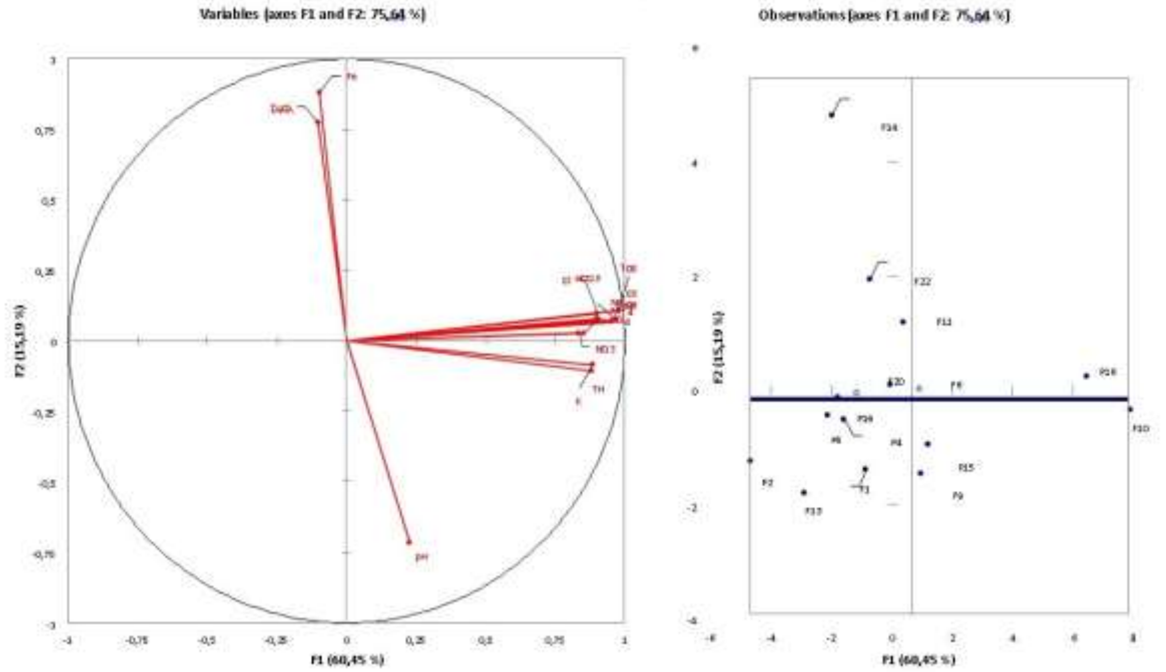

Figure 4. Principal component analysis biplot (Factor 1 vs. Factor 2) showing loadings of major ions and sample distribution. Factor 1 (42.3%) represents water-rock interaction; Factor 2 (21.4%) represents anthropogenic pollution (NO_3^-, Cl^-).

2.3 Microbiological Parameters

Bacteriological results revealed widespread but variable contamination: 81% of samples exceeded WHO limits for total coliforms (0-1.6×10^4 CFU/100 mL; mean $3.38\times10^3 \pm 4.5\times10^3$), and 38% for *E. coli* (0-4.32×10^3 CFU/100 mL; mean $3.28\times10^2 \pm 8.2\times10^2$), with aerobic mesophiles 10^2-10^5 CFU/mL. Counts were significantly higher in wells (median coliforms 1.2×10^3 vs. 150 in boreholes; $p < 0.001$, Wilcoxon rank-sum test) and in the wet season ($p = 0.03$, Wilcoxon signed-rank test), attributable to surface runoff and cracked linings. *E. coli* positivity correlated with latrine proximity ($r = -0.65$, $p < 0.01$), with hotspots in Matadjir (100% exceedance). This pattern confirms the vulnerability of shallow wells to surface-borne fecal contamination, particularly during rainfall events when infiltrating runoff transports pathogens from nearby sanitation facilities.

Table 3. Bacteriological counts (CFU/100 mL; n = 16)

Parameter	Min	Max	Mean ± SD	% Exceeding WHO
Total coliforms	0	1.6×10^4	$3.38\times10^3 \pm 4.5\times10^3$	81
E. coli	0	4.32×10^3	$3.28\times10^2 \pm 8.2\times10^2$	38

2.4 Integrated Quality Assessment: Potability and Irrigation Suitability

Chemical WQI scores ranged 25-145 (mean 72 ± 35), rating 81.25% (13/16) as good/excellent (<100), driven by compliant major ions but elevated TDS/EC in 25%. This indicates general chemical acceptability from a health perspective, although elevated salinity in a quarter of samples affects palatability. Bacteriological integration (coliform q_i >50 for 81%) yielded modified WQI >100 (poor) for 81%, with only 19% (3 boreholes) fully safe (overall WQI <100 and q-coliform ≤50). Sub-index breakdown: pH (q = 95-100), NO_3^- (q = 10-44, mean 10), EC (q = 4-100, mean 68).

Irrigation suitability was evaluated using SAR (0.5-4.2, mean 1.8 ± 1.0) and EC (61-2900 µS/cm, mean 629.7 ± 600 µS/cm) following USSL (1954) criteria. **Table 4** details the classification for all 16 samples: 25% (4/16) in C1S1 (low salinity, low sodium hazard), 43.75% (7/16) in C2S1 (medium salinity, low sodium hazard), 18.75% (3/16) in C3S1 (high salinity, low sodium hazard), and 12.5% (2/16) in C4S1 (very high salinity, low sodium hazard). All samples exhibit low sodium hazard (S1: SAR <10), suitable for most crops without soil degradation. Wells show significantly higher EC (median 450 µS/cm) than boreholes (median 250 µS/cm, p = 0.04, Wilcoxon rank-sum test), and the dry season exacerbates salinity (median 615 µS/cm vs. 270 µS/cm wet, p = 0.01, Wilcoxon signed-rank test). A positive correlation between EC and SAR (r = 0.65, p < 0.01, log-transformed) indicates partial coupling of salinization and sodium mobilization, particularly pronounced in wells during the dry season.

Complementary indices, such as permeability index (PI: 45-75%, mean 62 ± 10%) and residual sodium carbonate (RSC: <1.25 meq/L, mean 0.8), confirm good soil permeability and negligible alkalization risk (Table 4). These results suggest general suitability for irrigation with salt-tolerant crops like millet (EC <2000 µS/cm), but require rigorous management for sensitive crops (e.g., 20-30% yield loss for maize in C3S1 and C4S1 zones; Ayers & Westcot, 1985). The predominance of C2S1 (43.75%) indicates moderate viability, with precautions needed to minimize saline impacts on local agriculture.

Table 4. USSL classification and irrigation indices of groundwater in Abéché (n = 16)

Sample	Type	Season	EC (µS/cm)	SAR	USSL Class	Irrigation Risk	PI (%)	RSC (meq/L)	%Na	KR
1	**Well**	Dry	320	1.2	C2S1	Medium salinity, low sodium	62	0.8	28	0.4
2	**Well**	Wet	210	0.8	C1S1	Low salinity, low sodium	60	0.7	25	0.3
3	**Well**	Dry	890	2.1	C3S1	High salinity, low sodium	65	0.9	32	0.5
4	**Well**	Wet	650	1.8	C2S1	Medium salinity, low sodium	63	0.8	30	0.4
5	**Well**	Dry	2900	4.2	C4S1	Very high salinity, low sodium	70	1.0	45	0.6
6	**Well**	Wet	450	1.5	C2S1	Medium salinity, low sodium	61	0.8	28	0.4

7	**Well**	Dry	380	1.3	C2S1	Medium salinity, low sodium	62	0.7	26	0.3
8	**Borehole**	Wet	290	1.1	C2S1	Medium salinity, low sodium	60	0.6	24	0.3
9	**Borehole**	Dry	150	0.5	C1S1	Low salinity, low sodium	58	0.5	15	0.2
10	**Borehole**	Wet	180	0.7	C1S1	Low salinity, low sodium	59	0.6	20	0.2
11	**Borehole**	Dry	210	0.9	C1S1	Low salinity, low sodium	60	0.6	22	0.3
12	**Borehole**	Wet	250	1.2	C2S1	Medium salinity, low sodium	61	0.7	25	0.3
13	**Borehole**	Dry	610	2.8	C2S1	Medium salinity, low sodium	64	0.9	35	0.5
14	**Borehole**	Wet	720	3.1	C2S1	Medium salinity, low sodium	65	0.9	38	0.5
15	**Borehole**	Dry	830	3.5	C3S1	High salinity, low sodium	66	1.0	40	0.5
16	**Borehole**	Wet	950	3.9	C3S1	High salinity, low sodium	67	1.0	42	0.6

Indices calculated in meq/L; USSL zones per FAO (Ayers & Westcot, 1985). All SAR values <10 indicate S1 class.

3. Discussion

3.1 Controls on Groundwater Hydrochemistry and Seasonal Dynamics

The near-neutral to slightly alkaline pH (mean 6.9) and dominant Ca-Mg-HCO_3 facies align with carbonate dissolution in basement aquifers, where percolating rainwater (pH ~6.5, low TDS ~50 mg/L) equilibrates with calcite:

$$CaCO_3(s) + CO_2(aq) + H_2O \rightarrow Ca^{2+} + 2HCO_3^-$$

Saturation indices (SI_calcite ≈ 0.4, SI_dolomite ≈ 0.2) support this interpretation, indicating that groundwater is near equilibrium with carbonate minerals, consistent with active dissolution and precipitation dynamics (Appelo & Postma, 2005). The slight oversaturation of calcite in some samples may result from CO_2 degassing during sampling or evaporation. The rock-weathering dominance inferred from ion-TDS relationships (60-80% of samples) aligns with West African fractured systems (Abderamane, 2016; Toule et al., 2024; Zongo et al., 2024; Shuaibu et al., 2025). Mg^{2+} enrichment (mean 14 mg/L) likely stems from ferromagnesian silicates in gneisses, while dry-season EC peaks (up to 2900 µS/cm) reflect prolonged residence and evapotranspiration concentration under oxic conditions (DO mean 4.9 mg/L) that inhibit reduction. PCA Factor 1 (42.3% variance) validates this, with loadings tying HCO_3^-/Ca^{2+} to lithology and depth ($r = 0.68$). However, evaporation (inferred from Cl^-/HCO_3^- ratios >1 in dry samples) and minor ion exchange (BEI mean -1.2; Factor 3) contribute ~12% variance, often underestimated in semi-arid models but evident here via seasonal TDS spikes (+15% dry). The significant increase in EC and TDS during the dry season ($p < 0.01$) is primarily attributed to reduced recharge and concentrated evaporation, whereas wet-season flushing leads to dilution and a concomitant rise in nitrate from surface runoff.

Anthropogenic signatures in Factor 2 (21.4% variance) are pronounced: NO_3^- (mean 5 mg/L up to 22) and Cl^- (mean 21 mg/L) elevations correlate with latrine proximity ($r = -0.72$; distances 10-150 m), suggesting leachate infiltration via sandy soils (permeability ~10^{-4} m/s). Wet-season NO_3^- increases (+25%) suggest runoff transport and enhanced leaching from contamination sources, echoing Djaouda et al. (2013) in Cameroon and Berest et al. (2024) in Fitri, Chad, where similar fractured aquifers amplify pollutant migration (hydraulic conductivity ~10^{-5} m/s). The negative SI for gypsum (mean -1.8) rules out evaporite dissolution as a major source of SO_4^{2-}; instead, SO_4^{2-} may originate from oxidation of sulfide minerals or atmospheric deposition. Spatial kriging ($R^2 = 0.75$) maps hotspots in Matadjir (EC >1000 µS/cm, NO_3^- >10 mg/L), validating site selection criteria.

3.2 Mechanisms of Anthropogenic Contamination and Hydrogeological Controls

Shallow wells are particularly vulnerable to contamination due to local hydrogeological conditions. The unsaturated zone beneath wells is thin (typically <5 m in the study area), composed of sandy lateritic soils with high permeability, allowing rapid infiltration of surface contaminants. In contrast, boreholes tap deeper fractured zones where the overlying weathered layer provides some natural attenuation, though fractures can also act as preferential pathways if they intersect contaminated zones. The strong correlation between *E. coli* presence and latrine distance ($r = -0.65$) suggests a strong association between onsite sanitation and fecal contamination, though additional tracer studies (e.g., microbial source tracking) would be needed to confirm causality. During the wet season, rising water tables can directly connect the saturated zone with latrine pits, while surface runoff transports fecal matter from open defecation areas into wells (especially those without protective aprons). This seasonal pattern is consistent with observations in Niamey (Chippaux et al., 2002), where 90% of urban wells showed contamination after rains. The persistence of *E. coli* in oxic groundwater (DO >3 mg/L) suggests that bacterial survival is prolonged, possibly due to low competition and moderate temperatures (26-32°C). The co-transport of nitrate and bacteria ($r = 0.58$, $p < 0.05$) further supports a common source from fecal leachate.

3.3 Comparison with Regional Studies

Compared to neighboring regions, Abéché's groundwater exhibits similar geochemical signatures (Ca-Mg-HCO_3 facies, EC 200-1500 µS/cm) but higher microbial contamination. In Moussoro, Chad, Diallo et al. (2024) reported coliforms up to 10^3 CFU/100 mL but lower NO_3^- (<10 mg/L), likely due to lower population density and better sanitation. In Fitri, Bérest et al. (2024) found NO_3^- up to 15 mg/L and high coliforms, comparable to Abéché, reflecting similar sanitation deficits. In N'Djamena, Ousman et al. (2024) documented elevated trace metals and bacteriological contamination, attributing it to industrial and domestic waste. The higher coliform counts in Abéché wells compared to boreholes mirror findings in Niamey (Chippaux et al., 2002), where shallow wells were more vulnerable. The predominance of C2S1 irrigation water (43.75%) in Abéché is intermediate between the low-salinity waters of Moussoro (mostly C1S1) and the higher-salinity waters of some N'Djamena boreholes (C3S1). These differences may reflect local variations in geology, recharge rates, and anthropogenic pressure, though direct comparisons are complicated by differing sampling protocols and analytical methods between studies.

3.4 Implications for Climate Change and Long-Term Trends

Climate projections for the Sahel indicate increased aridity and more intense rainfall events (IPCC, 2022; WMO, 2025). Reduced recharge would further concentrate dissolved solids, potentially shifting more samples into higher salinity classes (C3-C4), thereby reducing irrigation suitability for salt-sensitive crops. Simultaneously, intense rainfall following dry periods can flush accumulated contaminants from the surface into groundwater, exacerbating seasonal peaks in microbial pollution. The observed dry-season EC increase (+15%) already hints at evaporative concentration; under a warmer climate, this effect could intensify. Therefore, sustainable management must account for these trends by promoting water conservation, enhancing recharge (e.g., through managed aquifer recharge), and implementing source protection measures.

3.5 Study Limitations and Future Research

The sample size (n = 16, power ~70%) may underestimate spatial heterogeneity, with ±15% uncertainty on means. Purposive selection prioritized vulnerability hotspots, which could limit generalizability to less affected areas, though it effectively captures worst-case scenarios. Absence of isotopic data ($\delta^{18}O$, $\delta^{2}H$) limits recharge source tracing and evaporation quantification. The microbiological analysis, limited to indicator organisms, may overlook specific pathogens (e.g., *Vibrio cholerae*, enteric viruses). Logistical constraints restricted sampling frequency.

Future research should expand to n ≥ 50 with quarterly sampling over multiple years, incorporate stable isotopes and age tracers (^{3}H, ^{14}C), and include pathogen-specific assays. DRASTIC vulnerability mapping could refine predictive models, and pilot interventions (e.g., solar disinfection, well improvement) should be tested for efficacy.

Conclusion

This study shows that groundwater in Abéché's unserved districts is chemically acceptable for drinking (81% WQI good/excellent, though 25% exceed palatability limits) but microbiologically unsafe (81% coliform exceedance, 38% *E. coli*), with irrigation suitability (43.75% C2S1) posing moderate risks to crop productivity. Geogenic processes (carbonate weathering) dominate mineralization, while anthropogenic factors, particularly latrine proximity and seasonal runoff, are strongly associated with contamination, as evidenced by PCA, saturation indices, and spatial mapping. Saturation indices confirm carbonate equilibrium and gypsum undersaturation, reinforcing geogenic control. Potential interventions to consider include: (1) establishing sanitation buffers (>50 m) where feasible, recognizing that land constraints may limit implementation in dense settlements; (2) promoting well aprons and fencing as low-cost protective measures; (3) exploring community-based chlorination options with proper training and monitoring; and (4) developing routine monitoring programs to track water quality trends. These measures, grounded in transparent data and hydrogeological insights, can enhance potability, public health, and agricultural resilience, advancing SDG 6 in arid urban settings.

References

Abderamane, H. 2016. Hydrogeochemical and isotopic characterization of the groundwater in the Dababa area (Chad). *African Journal of Environmental Science and Technology*, 10(1), 1-12. https://doi.org/10.5897/AJEST2016.2200

APHA 2025. *Standard methods for the examination of water and wastewater* (24th ed.). American Public Health Association.

Appelo, C. A. J., & Postma, D. 2005. *Geochemistry, groundwater and pollution* (2nd ed.). CRC Press. https://doi.org/10.1201/9781439833544

Ayers, R. S., & Westcot, D. W. 1985. *Water quality for agriculture* (FAO Irrigation and Drainage Paper 29 Rev.1). Food and Agriculture Organization.

Bérest, J., Ngounou Ngatcha, B., Mouhaman Arabi, A., Yalo, N., Valdes, D., Bila, D., Razack, M., & Mariko, A. 2024. Groundwater quality status in the Division of Fitri (Chad). *Sustainable Water Resources Management*, 10, 39. https://doi.org/10.1007/s40899-023-00994-0

BRGM 2010. *Hydrogeological map of Chad (Scale 1:2,000,000)*. Bureau de Recherches Géologiques et Minières. Retrieved March 15, 2026, from https://www.brgm.fr/en/reference-completed-project/hydrogeological-map-africa

Brown, R. M., McClelland, N. I., Deininger, R. A., & Tozer, R. G. 1970. A water quality index - Do we dare? *Water & Sewage Works*, 117(10), 339-343.

Chippaux, J. P., Houssier, S., Gross, P., Bouvier, C., & Brissaud, F. 2002. Pollution of the groundwater in the city of Niamey, Niger. *Bulletin of the World Health Organization*, 80(5), 390-395. https://doi.org/10.1590/S0042-96862002000500014

Diallo, F. A., Ngounou Ngatcha, B., Mahamat Nour, A. D., & Yalo, N. 2024. Sustainable management of drinking water quality in the locality of Moussoro (Chad). *Discover Water*, 4, 164. https://doi.org/10.1007/s43832-024-00164-z

Direction de la Météorologie, Tchad 2023. *Bulletin climatologique annuel 2023*. Ministère de l'Environnement, Tchad.

Djaouda, M., Njine, T., Liang, S., Ebang Menye, D., Gaké, B., Zebaze Togouet, S. H., & Nola, M. 2013. Survival and growth of Vibrio cholerae, Escherichia coli, and Salmonella spp. in well water used for drinking purposes in Garoua (North, Cameroon). *International Journal of Water Resources Development*, 29(2), 215-228. https://doi.org/10.1080/07900627.2012.721694

Esri 2023. *ArcGIS Desktop: Release 10.8* [Computer software]. Environmental Systems Research Institute. https://desktop.arcgis.com

Faul, F., Erdfelder, E., Lang, A. G., & Buchner, A. 2007. GPower 3: A flexible statistical power analysis program for the social, behavioral, and biomedical sciences. *Behavior Research Methods*, 39(2), 175-191. https://doi.org/10.3758/BF03193146

Gibbs, R. J. 1970. Mechanisms controlling world water chemistry. *Science*, 170(3962), 1088-1090. https://doi.org/10.1126/science.170.3962.1088

Hammer, Ø., Harper, D. A. T., & Ryan, P. D. 2001. PAST: Paleontological statistics software package for education and data analysis. *Palaeontologia Electronica*, 4(1), 4. https://palaeo-electronica.org/2001_1/past/issue1_01.htm

Hem, J. D. 1985. *Study and interpretation of the chemical characteristics of natural water* (3rd ed., U.S. Geological Survey Water-Supply Paper 2254). U.S. Geological Survey. https://doi.org/10.3133/wsp2254

Horton, R. K. 1965. An index number system for rating water quality. *Journal of the Water Pollution Control Federation*, 37(3), 300-306.

Institut National de la Statistique, Tchad 2021. Résultats définitifs du 3ème Recensement Général de la Population et de l'Habitat (RGPH-3). Ministère de l'Économie et du Développement, Tchad.

IPCC 2022. *Climate Change 2022: Impacts, Adaptation, and Vulnerability*. Contribution of Working Group II to the Sixth Assessment Report of the Intergovernmental Panel on Climate Change. Cambridge University Press. https://doi.org/10.1017/9781009325844

Koné, B. 2005. Hydrogeochemical evolution of basement aquifers in Côte d'Ivoire. *Hydrological Sciences Journal*, 50(3), 479-495. https://doi.org/10.1623/hysj.2005.50.3.479

Ministry of Water and Energy, Chad 2022. *National water resources master plan*. Government of Chad.

Ngounou Ngatcha, B. 2011. Groundwater resources in semi-arid basement terrains of Central Africa. *Proceedings of the IAH Congress*, 18, 45-56.

Nour, A. M., Djibrine Mahamat, A., Mahamat Nour, A. D., & Yalo, N. 2024. Assessment of the microbiological quality of drinking water from some wells and boreholes in the city of Abéché (Chad). *Food and Nutrition Sciences*, 15(12), 1381-1395. https://doi.org/10.4236/fns.2024.1512004

Ousman, M. A. H., Ngounou Ngatcha, B., Mahamat Nour, A. D., & Yalo, N. 2024. Groundwater quality assessment for drinking and agricultural purposes under arid climate in N'Djamena, Chad. *Groundwater for Sustainable Development*, 26, 101312. https://doi.org/10.1016/j.gsd.2024.101312

Parkhurst, D. L., & Appelo, C. A. J. 2013. Description of input and examples for PHREEQC version 3A computer program for speciation, batch-reaction, one-dimensional transport, and inverse geochemical calculations (U.S. Geological Survey Techniques and Methods, Book 6, Chap. A43). U.S. Geological Survey. https://doi.org/10.3133/tm6A43

R Core Team 2023. *R: A language and environment for statistical computing* [Computer software]. R Foundation for Statistical Computing. https://www.R-project.org/

RockWare 2012. *AqQA (Version 1.1.5)* [Computer software]. RockWare Inc. https://www.rockware.com/product/aqqa/

Sambo, A. M., Ngounou Ngatcha, B., Mahamat Nour, A. D., & Yalo, N. 2023. Groundwater resources of the transboundary Quaternary aquifer of the Lake Chad Basin: Towards a better management via isotope hydrology. *Resources*, 12(12), 138. https://doi.org/10.3390/resources12120138

Shuaibu, A., Kalin, R. M., Phoenix, V., & Banda, L. C. 2025. Investigation of groundwater recharge in the transboundary Komadugu-Yobe basin, Nigeria via stable isotopes of δ18O and δ2H and comparison with the wider Sahel, Africa. *Science of the Total Environment*, 994, 180043. https://doi.org/10.1016/j.scitotenv.2025.180043

Toulé, K. B., Ngounou Ngatcha, B., Mahamat Nour, A. D., & Yalo, N. 2024. Hydrogeochemistry and water quality index for groundwater sustainability in basement aquifers: A case study in the Kolokani area (Mali). *Water*, 16(4), 601. https://doi.org/10.3390/w16040601

UN-Habitat 2022. *The state of African cities 2022: Reimagining urban planning and financing for a resilient future*. United Nations Human Settlements Programme. https://unhabitat.org/the-state-of-african-cities-2022

USSL 1954. *Diagnosis and improvement of saline and alkali soils* (USDA Handbook No. 60). U.S. Department of Agriculture. https://www.ars.usda.gov/ARSUserFiles/20360500/hb60_pdf/hb60complete.pdf

Vassolo, S., Ngounou Ngatcha, B., Mahamat Nour, A. D., & Yalo, N. 2023. Groundwater recharge processes in the Lake Chad Basin based on isotopic and chemical data. *Hydrogeology Journal*, 31(8), 2457-2475. https://doi.org/10.1007/s10040-023-02699-2

WHO 2011. *Guidelines for drinking-water quality* (4th ed.). World Health Organization. https://www.who.int/publications/i/item/9789241549950

WHO 2022. *World health statistics 2022: Monitoring health for the SDGs, sustainable development goals*. World Health Organization. https://www.who.int/publications/i/item/9789240051157

WHO/UNICEF 2025. *Progress on household drinking water, sanitation and hygiene 2000-2024: Special focus on inequalities*. WHO/UNICEF Joint Monitoring Programme. https://www.who.int/publications/m/item/progress-on-household-drinking-water-sanitation-and-hygiene-2000-2024---special-focus-on-inequalities

WMO 2025. *State of the global climate 2024* (WMO-No. 1368). World Meteorological Organization. https://wmo.int/publication-series/state-of-global-climate-2024

Yacouba, A., Schamper, C., Valdes, D., Moussa, I., Ramel, D., & Mariko, A. 2024. Integrating geological, hydrogeological and geophysical data to identify groundwater resources in granitic basement areas (Guéra Massif, Chad). *Hydrogeology Journal*, 32(3), 759-772. https://doi.org/10.1007/s10040-024-02766-2

Zongo, A., Keita, A., Ngounou Ngatcha, B., Mahamat Nour, A. D., & Yalo, N. 2024. Hydrogeochemical processes in basement areas using principal component in Burkina Faso (West African Sahel). *Journal of Environmental & Earth Sciences*, 7(1), 1-15. https://doi.org/10.30564/jees.v7i1.6932

Author contributions:
Hammadou Abdou: Conceptualization, Methodology, Supervision, Writing - review & editing
Moustapha Dinar Ibrahim: Conceptualization, Methodology, Formal analysis, Investigation, Writing - original draft, Writing - review & editing, Visualization, Project administration, Corresponding author
Abdelhamid Mahamat Issa: Methodology, Investigation, Data curation, Formal analysis
Laokoura Charles: Methodology, Software, Formal analysis, Validation
Mahamat Nour Abdelhakh Safi: Investigation, Data curation, Resources, Validation

AI usage statement:
AI was used solely to reformat the reference list into the journal's citation style. No AI was used for data analysis, interpretation, or generation of scientific content. The authors assume full responsibility.

Acknowledgements:
The authors acknowledge the support of the Department of Geology at Adam Barka University of Abéché and the University of N'Djamena for providing equipment and logistical support during fieldwork and laboratory analyses. We also thank the local authorities and communities in Abéché for their assistance and cooperation during the field data acquisition. Special thanks to the National Water Laboratory (LNE), N'Djamena, for conducting the physicochemical and bacteriological analyses.

Funding source:
No funding was received to assist with the preparation of this manuscript.

Declaration of competing interest:
The authors declare that they have no known competing financial interests or personal relationships that could have appeared to influence the work reported in this paper.